Reconstructing the Mediaeval low stands of Mono Lake, Sierra Nevada, California, USA

Nicholas E. Graham and Malcolm K. Hughes

The Holocene 2007; 17; 1197
DOI: 10.1177/0959683607085126

The Holocene 17,8 (2007) pp. 1197–1210

Reconstructing the Mediaeval low stands of Mono Lake, Sierra Nevada, California, USA

Nicholas E. Graham[1,2,*] and Malcolm K. Hughes[3]

([1]Scripps Institution of Oceanography, La Jolla CA, USA; [2]Hydrologic Research Center, 12780 High Bluff Drive Suite 250, San Diego CA 92130, USA; [3]Laboratory for Tree-Ring Research, University of Arizona, 105 West Stadium, Tucson AZ 85721-0058, USA)

Received 8 January 2007; revised manuscript accepted 27 July 2007

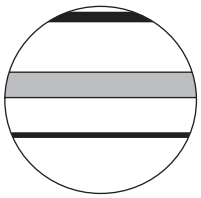

Abstract: Palaeosimulations of Mono Lake covering the past 2 kyr have been conducted using a water balance model forced with tree-ring derived inflow estimates. The results show two low stands, during the ninth to tenth and twelfth to thirteenth centuries, that agree well in timing and magnitude with those described by Stine (1987, 1990, 1994) on the basis of geomorphic evidence and relict trees and shrubs exposed on Mono Lake's artificially exposed shorelands. The lake simulation provides independent corroboration of the timing and magnitude of Stine's drought-induced low stands and supports the accuracy of tree-ring-derived estimates of Mediaeval precipitation and runoff reductions in the central Sierra Nevada. Specifically, we estimate that during the two Mediaeval droughts, centennial average precipitation and river runoff in the central Sierra Nevada reached as low as 75% of the twentieth century values, with multidecade averages as low as 60–65%. In both magnitude and duration, these droughts far exceed anything experienced in the region during modern times. An analysis of the spatial patterns of reconstructed drought indices shows that the particular 'two drought' Mono Lake low stand signal was focused over central and southern California, indicating the dominant role of boreal winter precipitation deficits. In this respect, the 'Great Sierra Nevada droughts' were somewhat distinct from the more general Great Basin/far western Plains pattern of Mediaeval aridity over the western USA.

Key words: Mediaeval droughts, Mono Lake, Sierra Nevada, California, low stands, runoff, water balance model, lake shorelines, dendrochronology, environmental reconstruction.

Introduction

Mono Lake is a large (~20 000 ha) terminal lake located just east of the crest of the central Sierra Nevada (California; 37.95°N 119.11°W) with a modern natural surface elevation of about 1955 m. Lacking outflow, changes in lake volume are determined by the balance between evaporation and inflows (runoff and precipitation), with approximately 77% of the modern inflow occurring in the form of runoff from Sierra snowmelt (Vorster, 1985) and the remainder as precipitation and groundwater flow into the lake. Nearly all of the inflow ultimately derives from North Pacific storms during the boreal winter half of the year.

Early in the1940s, the City of Los Angeles began diverting water from the streams flowing into Mono Lake for municipal water supply, causing lake levels to fall. During the early 1960s, by which time the lake had fallen by about 6 m from its pre-diversion level, water resource engineer Sydney Harding and ecologist Donald Lawrence noted relict stumps rooted along the artificially exposed shorelands, remains of trees and shrubs that lived at times when the lake was below pre-diversion levels (Lawrence and Lawrence, 1961; Harding, 1965). Developing these findings, Stine (1987, 1990, 1994, 1998) investigated the chronology and context of the relict vegetation and other proxy data at Mono Lake and other nearby sites (including Tenaya Lake, West Walker River, Osgood Swamp, Owens Lake and Walker Lake).

Stine's (1987, 1990, 1994) results from Mono Lake (supported by those from the other sites noted above) were based on a synthesis of several types of evidence. These include sedimentary regressive and transgressive sequences exposed on feeder stream channels, lake margin geomorphic features, elevations and ^{14}C-derived death dates of relict vegetation and tree-ring ages of exposed stumps. This evidence indicates the occurrence of two major Mediaeval droughts and associated Mono Lake low stands, the first during the tenth and eleventh centuries and the second during the twelfth to thirteenth centuries. These droughts were severe enough to cause Mono Lake level to drop approximately 17 m below today's calculated 'natural level' (Vorster, 1985).

*Author for correspondence (e-mail: ngraham@hrc-lab.org)

10.1177/0959683607085126

Stine's (1987, 1990) evidence for regional Mediaeval drought in the Sierra Nevada and western Nevada was consistent with earlier tree-ring evidence indicating a multicentury period of marked aridity in the western USA (LaMarche, 1974; Stockton and Meko, 1975). The character and duration of this 'Mediaeval Climate Anomaly' (MCA; a designation suggested by Stine (1994) as more widely appropriate than 'Mediaeval Warm Period') has since been corroborated by many studies using a wide variety of proxy records (eg, Mehringer and Wigand, 1990; Graumlich, 1993; Swetnam, 1993; Arbogast, 1996; Hughes and Graumlich, 1996, Anderson and Smith, 1997, Hughes and Funkhouser, 1998; Mohr *et al*., 2000; Byrne *et al*., 2001, Meko *et al*., 2001; Benson *et al*., 2002, Cook *et al*., 2004, Yuan *et al*., 2004, Graham *et al*., 2006).

Two of the studies noted above focused on Great Basin terminal lakes other than Mono Lake that receive most of their input from the Sierra Nevada. Benson *et al*. (2002), using evidence from lake sediment cores from Pyramid Lake (about 160 km north of Mono Lake), relict trees and tree-rings, inferred a series of droughts in the Sierra Nevada after 1200 yr BP. Yuan *et al*. (2004) analysed sediment cores from Walker Lake (approximately 100 km north-northeast of Mono Lake), inferring generally dry conditions from AD 1000–1360 and noting suggestions of agreement with the timing of the Mono Lake low stands. Dating uncertainties and the characteristics of their principal proxy ($\delta^{18}O$) preclude definitive matching of these records with the Mono Lake low stands.

Meko *et al*. (2001) produced a multicatchment tree-ring-based reconstruction of total Sacramento River flow extending back to the ninth century AD. Low flow episodes associated with the Mono Lake low stands do not appear in this reconstruction (although the MCA does appear as an extended period of moderately low flows). One possible reason for this is that the Sacramento River catchment covers most of northern California, an area much larger than the central Sierra Nevada catchment of Mono Lake and all of which is not always in climatological synchrony with the central Sierra Nevada. A second and related reason is that for the pre-AD 1100 part of the Meko *et al*. reconstruction, the northern Sacramento Basin is represented by one tree chronology from central Oregon. This record indicates relatively moist conditions during the droughts associated with Mono Lake low stands (the lack of arid conditions in far Northern California and Oregon at this time is supported the drought index data of Cook *et al*. (2004) used in the present study that indicates near normal conditions (see Figure 10) in central Oregon).

While the case for widespread aridity in the western USA during Mediaeval times is well established and the evidence for the Mono Lake low stands is clear, questions remain concerning the severity, timing and spatial extent of the specific droughts associated with the low stands. One central question we address is whether climatic conditions persistently severe enough to have driven Mono Lake to its Mediaeval low stand levels can be confirmed from a tree-ring-derived streamflow reconstruction for Merced River on the western slope of the Sierra immediately east of Mono Lake. The investigation takes advantage of several intersecting approaches and lines of evidence.

- The water budget of Mono Lake has been studied extensively and is well understood (Vorster, 1985), so that the lake's response to changes in inflow can be estimated using a well-tested modelling approach.
- The timing of the Mono Lake low stand onsets and (especially) terminations at particular elevations are known within radiocarbon accuracy (50–75 years).
- The levels of the Mono Lake low stands are known to within ± 0.5 m from sedimentary and geomorphic evidence.
- Nearly all of the inflow (runoff and precipitation) to Mono Lake derives from cool-season storms off the North Pacific. Streams on the western side of the Sierra derive their inflow from these same storms.
- Variability in measured Sierra Nevada snowmelt runoff into Mono Lake agrees closely ($R = 0.95$ for 1937–83) with that in a longer record from the adjoining catchment (Merced River) on the western side of the Sierra Nevada.
- Tree-ring data can be used to produce a reasonably accurate reconstruction ($R = 0.82$) of twentieth-century Sierra Nevada streamflow, and presumably for the last 1000–2000 years.

Specifically, we use a water balance model (following Vorster, 1985) driven with reconstructed inflow to perform palaeosimulations of Mono Lake. The reconstructed inflows are derived from regional tree-ring data and are calibrated with Merced River discharge and Mono Lake precipitation data. We also consider the extent and spatial pattern of droughts associated with the Mono Lake low stands. The goal of the work is to provide a clearer, physically consistent and more quantitative idea of the character of the Mediaeval climatic change over the far western USA.

The section 'Water budget, models and data' below provides some background on the water budget of Mono Lake and the water balance model, describes the configuration of the water budget model as used in this work and the various data sets used. The following section presents the results, and the final section provides a short summary.

Water budget, models and data

Water budget and water balance model

The declines of Mono Lake during the 1950s–1970s and the increasing inflow diversions by the City of Los Angeles raised questions concerning inflow volumes required to stabilize the lake at various elevations. As part of the effort to investigate this issue, Vorster (1985) reviewed what was known about the lake's hydrology and water budget. He also assembled available measured streamflow, evaporation and precipitation data and estimated related data that were not directly available. Using the results of this work, Vorster created a water balance model for Mono Lake that closely tracked observed changes in lake level (ie, storage) from the 1930s–1980s, and clearly demonstrated that the inflow withdrawals by the City of Los Angeles were responsible for the declining lake levels. In the work described here, we apply Vorster's water balance modelling approach to produce a dynamical time-evolving simulation of the MCA Mono Lake low stands (as discussed later, Stine, 1987, 1990, applied the Vorster, 1985 model to calculate inflow reductions required for equilibrium lake levels). In the following paragraphs, we review basic aspects of the Mono Lake water budget, drawing much from the presentation in Vorster (1985).

On average, approximately 82% of the total Mono Lake inflow (precipitation, streamflow, groundwater flow) is in the form of runoff (streamflow and groundwater flow), with the other 18% coming from precipitation into the lake or onto adjacent land. Of the runoff, approximately 89% is from Sierra Nevada snowmelt, 80% of that is treated as measured flow (designated SNGR, Sierra Nevada Gauged Runoff). An additional portion of the Sierra Nevada runoff occurs in ungauged streams and is treated as an additional fixed fraction (about 11%) of SNGR (this portion is designated USR, Ungauged Sierra Runoff).

SNGR is composed of runoff from nine streams for which measurements are available over the 1937–1983 period covered in the Vorster (1985) simulations (three streams, Rush Creek, Lee Vining Creek and Mill Creek, account for approximately 90% of SNGR). The catchments of the streams in the SNGR group range along the crest of the Sierra Nevada, with more than half their

composite area above 3000 m m.s.l. A number of smaller streams for which measurements have been sporadic or do not exist make up the USR fraction. Runoff from Sierra snowmelt (SNGR and USR) is concentrated in late spring and early summer, with two-thirds occurring between May and July, and accounts for 73% of the total Mono Lake inflow.

The remaining 11% of Mono Lake runoff is in the form of groundwater flow (denoted NSR, non-Sierra runoff) that arises principally from infiltration of precipitation and streamflow (only sporadic gauge data exists for some streams in this area) into cracks and fissures in volcanic rock to the north, east and south of Mono Lake. Because it percolates through the bedrock before contributing to Mono Lake volume, NSR is assumed to vary slowly in time and is treated as a constant in the Vorster (1985) model. NSR accounts for an average of approximately 9% of the total Mono Lake inflow.

Precipitation, which provides the remaining 18% of total inflow into Mono Lake, comes primarily from winter storms propagating eastward from the Pacific, with approximately 80–85% of the annual total occurring between October and May. Most of the precipitation contribution to inflow is in the form of rain or snowfall directly into the lake (denoted Mono Lake Precipitation, MLP). The MLP provides 14% of total Mono Lake inflow and constitutes 78% of the precipitation contribution to total inflow.

To develop the MLP record, Vorster (1985) constructed an isohyet map of average annual precipitation for the Mono Lake catchment using measurements from regional precipitation gauges, along with snow depth and snow water equivalent observations from the Sierra. The long-term average annual precipitation rate into Mono Lake ($MLPR_A$) was calculated from the isohyet map. Year-to-year precipitation variability of MLP was calculated using an index (PI) derived from the long precipitation record from nearby Cain Ranch. This index is defined as the ratio of annual precipitation at Cain Ranch for a given year to the long-term annual average precipitation (at Cain Ranch). The total volumetric precipitation into Mono Lake (for year i) is then calculated by applying PI to the estimated long-term average Mono Lake precipitation (rate) and then multiplying by lake area (A_L) for that year (ie, $MLP_{(i)} = PI_{(i)} \times MLPR_A \times A_L$).

Precipitation onto the area surrounding the lake (denoted NLSP – Net Land Surface Precipitation) contributes the remainder of the Mono Lake inflow budget, accounting for 4% of the total inflow (22% of the precipitation contribution). NLSP is a 'net' term and includes the large fraction of the total precipitation lost in evapotranspiration from the surface and vegetation.

In a natural setting, evaporation (including evapotranspiration from plants) is the only means for water to leave the Mono Lake catchment, and thus at steady state lake evaporation balances inflow. By far the largest fraction of the evaporation volume (90% in the Vorster, 1985 simulations) is from the surface of Mono Lake (denoted MLE – Mono Lake Evaporation). Evaporation is maximized in the late summer and fall when lake temperatures are highest. In the Vorster (1985) model, the long-term average fresh water equivalent lake surface potential evaporation rate (MLPE = 114.3 cm/yr) and annual evaporation rate variability are estimated on the basis of evaporation pan measurements from local and regional sites (with adjustments for pan coefficients and biases between lake and pan energy balances). The fresh water equivalent evaporation rates are then adjusted for salinity (which alters the vapour pressure at the surface of the water) using a factor, ζ, that is a function $[g(V)]$ of lake volume (when the volume is low, salinity is high and the actual evaporation rate is lowered). The resulting rate is applied to lake area to obtain MLE.

In the Mono Lake palaeosimulations described in this paper, MLPE is set to a fixed value of 120.7 cm/yr (this value, slightly higher than used in the Vorster, 1985 model, was used to counter a slight (2 m) high bias in simulated modern 'natural' lake levels in our implementation of the Vorster, 1985 model). Using this value, MLE accounts for 92% of the total losses from the lake in a 'natural' twentieth-century setting.

A second evaporative loss term used in the Vorster (1985) model accounts for evaporation from bare ground in exposed areas around the lake (denoted BGE – Bare Ground Evaporation). The methods for accounting for this term are somewhat complicated, incorporating the changing areas of the exposed ground as lake level changes and time dependent parameterizations for the gradual evaporation of ground water. BGE accounted for between 0 to 8% per year of total evaporation in the Vorster (1985) simulation. For our simulations BGE was set to a fixed value appropriate for relatively low lake levels (6% of evaporation in a modern setting).

The Vorster (1985) model includes several terms for evapotranspiration losses (ETR), including those from riparian vegetation, irrigated pasture and non-irrigated (non-riparian) phreatophytes growing near springs and in low salinity areas with high water-table. These terms are rather modest, together accounting for an average of about 2% of the total losses in the Vorster (1985) simulations. The magnitudes of these terms have changed because of human impacts during the twentieth century (more pasture, less riparian vegetation and phreatophytes). The ETR losses are treated as fixed in the simulations presented here, using a value appropriate for the early twentieth century (Vorster, 1985; see Appendix A).

The Vorster (1985) model includes a number of artificial and modified natural water transfers (most importantly, losses to the Los Angeles diversions). Most of these were eliminated for the simulations presented here (see Appendix A for details).

A final necessary element of the model is a function relating lake volume (V), to lake level (Z) and lake area (A), $[Z, A] = g(V)$. For our simulation we use the functions given in Vorster (1985).

To summarize, the simulations conducted here used the water balance modelling approach of Vorster (1985) (with some modifications):

$$\sigma V = (\mathrm{SNGR} + \mathrm{USR} + \mathrm{NGR}) + (\mathrm{MLP} + \mathrm{NSLP}) - \mathrm{MLE} - \mathrm{ETR} - \mathrm{GLE}$$

$$V_t = V_{t-1} + \delta V$$

$$\mathrm{MLE} = \zeta E A$$

$$\zeta = g(V_t)$$

$$[Z, A] = f(V_t)$$

where σV represents the annual change in volume, V_t is the volume for a given year, and the other terms are defined in the text.

Data

Merced River (Pohono Bridge) discharge

The Merced River catchment is on the western side of the Sierra Nevada directly west of Mono Lake and the high-elevation portions of the two catchments share common boundaries along the crest of the Sierra Nevada. The Merced River flow record (designated Q_{MER}) used here is from the United States Geological Survey (USGS) Pohono Bridge gauge in Yosemite Valley, California (37°43′01″N,119°39′55″W; 1177 m m.s.l.), available from the California Data Exchange Center (http://cdec.water.ca.gov, last accessed 22 September 2007). The monthly record was used to construct an annual resolution water-year (October–September) discharge record covering 1901–1994.

Yosemite Valley precipitation

These data come from the US National Park Service gauge at Yosemite Park Headquarters in Yosemite Valley (37°44′24″ 117°34′59″, 1208 m m.s.l.) about 5 km from the Pohono Bridge gauge. This monthly record has been processed to provide

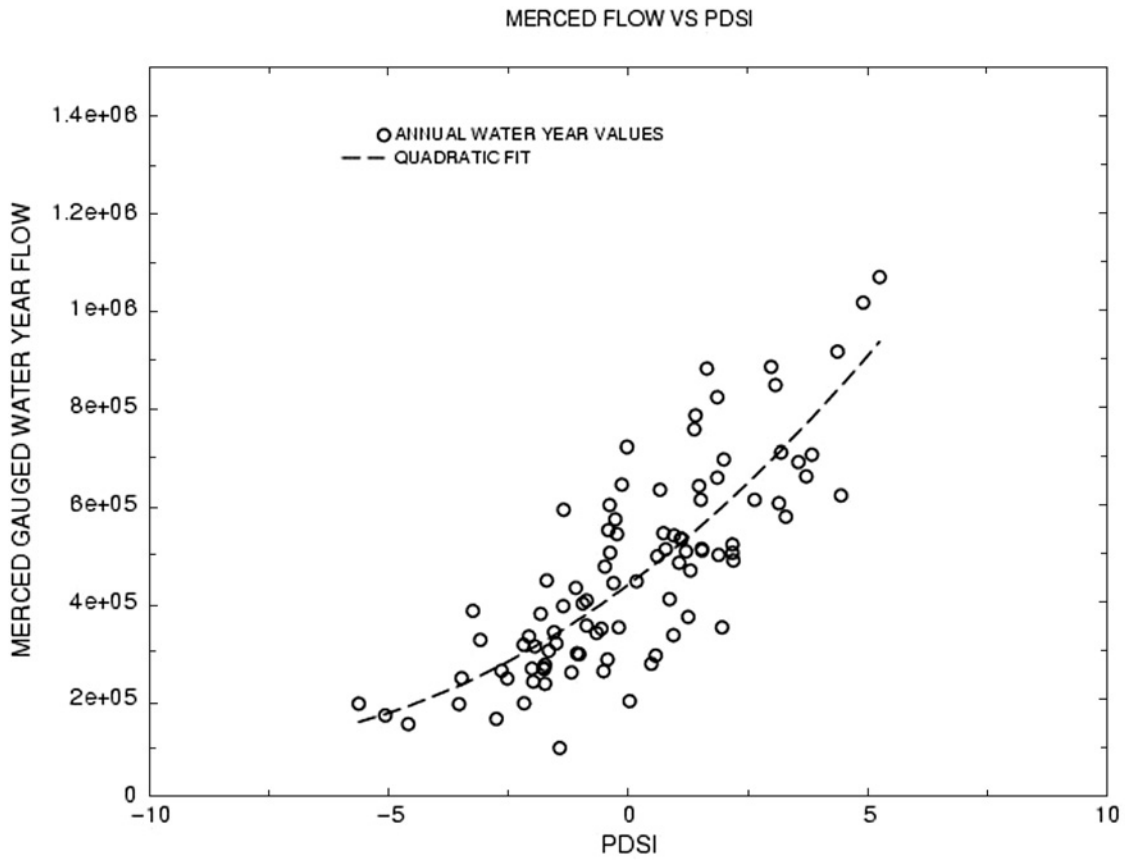

Figure 1 Merced River (Pohono Bridge) discharge (vertical axis) plotted as a function of reconstructed PDSI for the grid square centred at 37.5°N 120°W from the data set of Cook *et al*. (2004; circles, denoted SNDI in the text); data are for the period 1903–1994. The quadratic fit used to reconstruct Merced River flow is shown by the dotted line

water-year precipitation for the period 1907–2004. These data are available from the California Data Exchange Center (http://cdec.water.ca.gov).

West Walker River discharge

The flow record for the West Walker River comes from the USGS/California Department of Water Resources gauge at Coleville, CA (38°22′41″N 119°26′56″W, 2009 m m.s.l.; data available from http://cdec.water.ca.gov).

Mono Lake runoff, precipitation and potential evaporation

The Sierra Nevada gauged runoff (SNGR), precipitation (MLP) and potential evaporation (MLPE) records are available for 1937–1983 in Vorster (1985; see Section 'Water budget and water balance model'). To derive a Mono Lake precipitation rate record (MLPR), the MLP record was divided by the simulated Mono Lake area, also available in Vorster (1985). The Mono Lake potential evaporation record (MLPE) is available in Vorster (1985).

Central Sierra Nevada reconstructed Palmer Drought Severity Index (PDSI)

This record comes from the gridded tree-ring-based reconstruction of PDSI described by Cook *et al*. (2004). PDSI is an index of meteorological drought calculated from precipitation, temperature and available soil water data. Its use as a reference variable for large-scale drought reconstructions using tree rings was initiated by Meko *et al*. (1993) and developed further by Cook *et al*. (1996, 1999, 2004).

The reconstructed PDSI time series used in the present paper is for the 2.5° by 2.5° latitude-longitude grid square centred at 37.5°N 120°W (designated Sierra Nevada Drought Index, SNDI). The primary data from which the PDSI values were derived in the western USA are millennial moisture sensitive tree-ring chronologies, most developed at the University of Arizona Laboratory of Tree-Ring Research. Although the PDSI data reflect summer growing conditions, for the western USA and northern Mexico, winter half-year precipitation is the dominant factor controlling tree-ring-inferred summer PDSI variability. Dating in this record is precise and annual.

Results

Merced River flow reconstruction

The Merced River (Pohono Bridge) discharge record (Q_{MER}) and related reconstructions form one important basis for the Mono Lake simulations that follow. Merced River discharge (Q'_{MER}) was reconstructed by calibrating the observed Pohono Bridge discharge record with the reconstructed central Sierra Nevada drought index (SNDI) over the modern record. The Pohono Bridge data were used for calibration instead of the Mono Lake gauged inflow data (SNGR) because the former allows a much longer calibration period and because it closely tracks variability in the SNGR record over the period of overlap (see later discussion).

Figure 1 shows the scatter plot of SNDI and Q_{MER} for the 94-yr period 1900–1901 to 1993–1994. The positive and non-linear association between the two variables is apparent with the tree-ring index becoming increasingly (decreasingly) sensitive as flow decreases (increases). A quadratic least-squares regression was fit using these data (see Figure 1) giving the equation for the reconstructed flow as:

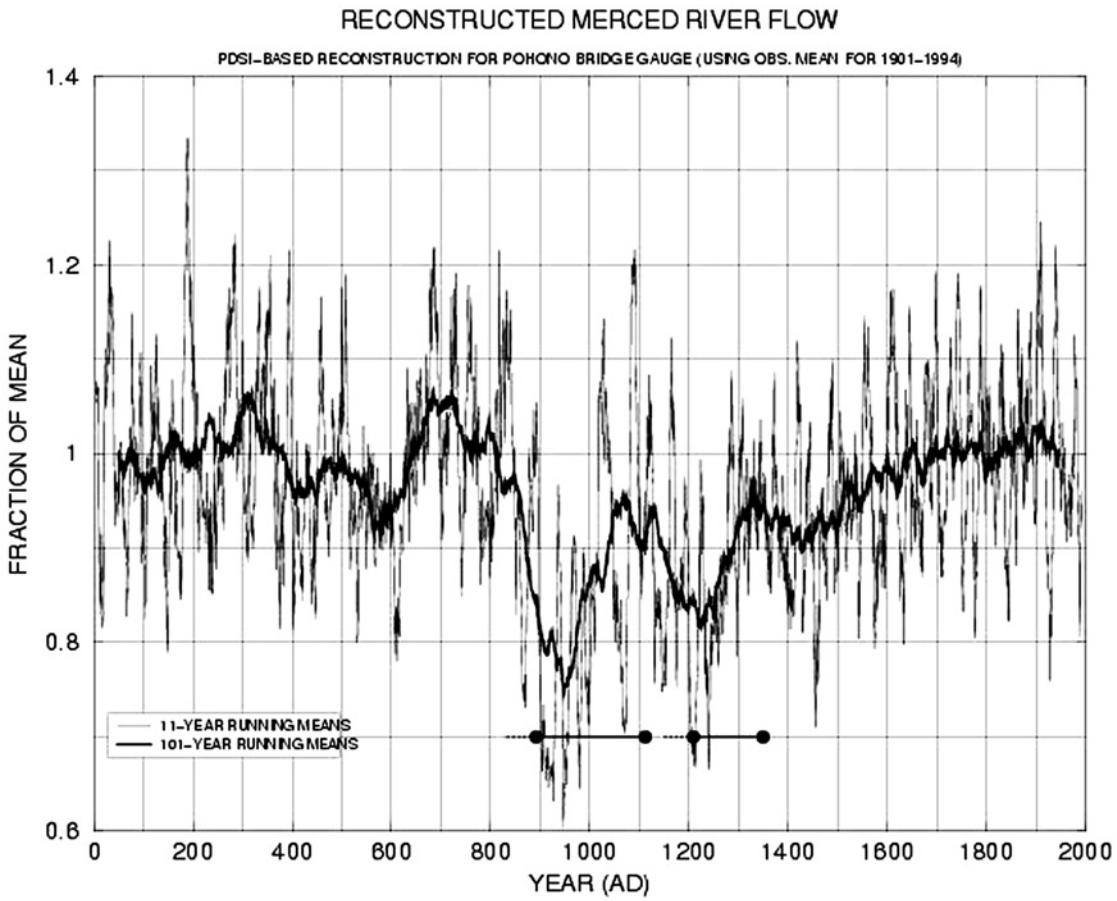

Figure 2 PDSI-based reconstruction of water-year Merced River flow plotted in terms of fraction of annual water-year mean over the 1900–1994 period of record. Solid thin line shows the 11-yr running mean; heavy line shows the 101-yr running mean. Solid lines with circles (and dashed extensions) indicate approximate duration of the Mediaeval Mono Lake low stands documented by Stine (1987, 1990, 1994)

$$Q'_{MER} = 2.076*10^6\ SNDI^2 + 9.081\times10^7\ SNDI + 5.358*10^8 \quad (1)$$

The correlation for this fit over the calibration period is 0.81 (a linear fit yields a correlation of 0.80 and larger residuals for extreme annual flows).

The stability of the regression model described above was examined using a cross-validation procedure in which individual years were sequentially deleted from the SNDI and Q_{MER} records, recalculating the regression between records with the one year deleted, and then estimating the value for the deleted year. (The deletion of a single year is justified by the lag 1-yr autocorrelations of 0.09 and 0.00 for the two data sets, respectively, for 1901–1994). The linear correlation between the observed Q_{MER} record and the cross-validated estimates is 0.80, establishing the stability of the regression procedure for the modern record.

Additional analyses were conducted to investigate the degree to which low frequency variance was retained in the reconstructed Merced flow record. Cross-spectral analysis (not shown) between the reconstructed and measured Merced River flow records show high coherence-squared values and near-zero phase for frequencies as low as one cycle per 30 years (the lowest frequency used), suggesting that variability is retained at least out to those timescales (though it is recognized that there is some artificial skill because both the reconstructed SNDI and the regressed flow estimates derive from their calibration periods). A similar analysis covering a longer period of time (1850–1998) was conducted using reconstructed PDSI from the grid square centred near San Francisco and the San Francisco historical precipitation record (using a quadratic fit of the PDSI to the precipitation record ($R = 0.70$)). In this case, the coherence square values indicate some loss of variability in the reconstruction for frequencies longer than about 30 years. It is not clear whether this result from the less moisture stressed coastal regions is relevant to the Sierra Nevada, and there are numerous other uncertainties involved in the various procedures and data, so it is not possible to say with assurance the degree to which low frequency variability is retained in the reconstructed Merced River flow record. Based on the results described above, and the fact that the regression procedure will result in loss of variance in any case, it seems likely that any bias in the low frequency content of the reconstructed flow record would be towards diminished signal.

Figure 2 shows the PDSI-derived reconstructed Merced River flow record developed as described above, converted to fractions of the modern (1901–1994) water-year average, then smoothed with 101-yr and 11-yr running means. The record shows two periods of especially low flow during Mediaeval times whose timing corresponds approximately to the Mono Lake low stands documented by Stine (1987, 1994). The first period begins with a very sharp drop in reconstructed flow during the ninth century, reaches a minimum in the tenth century, and recovers during the late eleventh and early twelfth centuries. The second low-flow period begins during the twelfth century and continues into the thirteenth century. Centennial averaged reconstructed flow reaches as low as 75% of the modern mean during the first minimum, with decadal values reaching about 60% of the modern mean. The second minimum in reconstructed flow is not so severe in terms of centennial averages (reaching 81% of the modern mean), though some

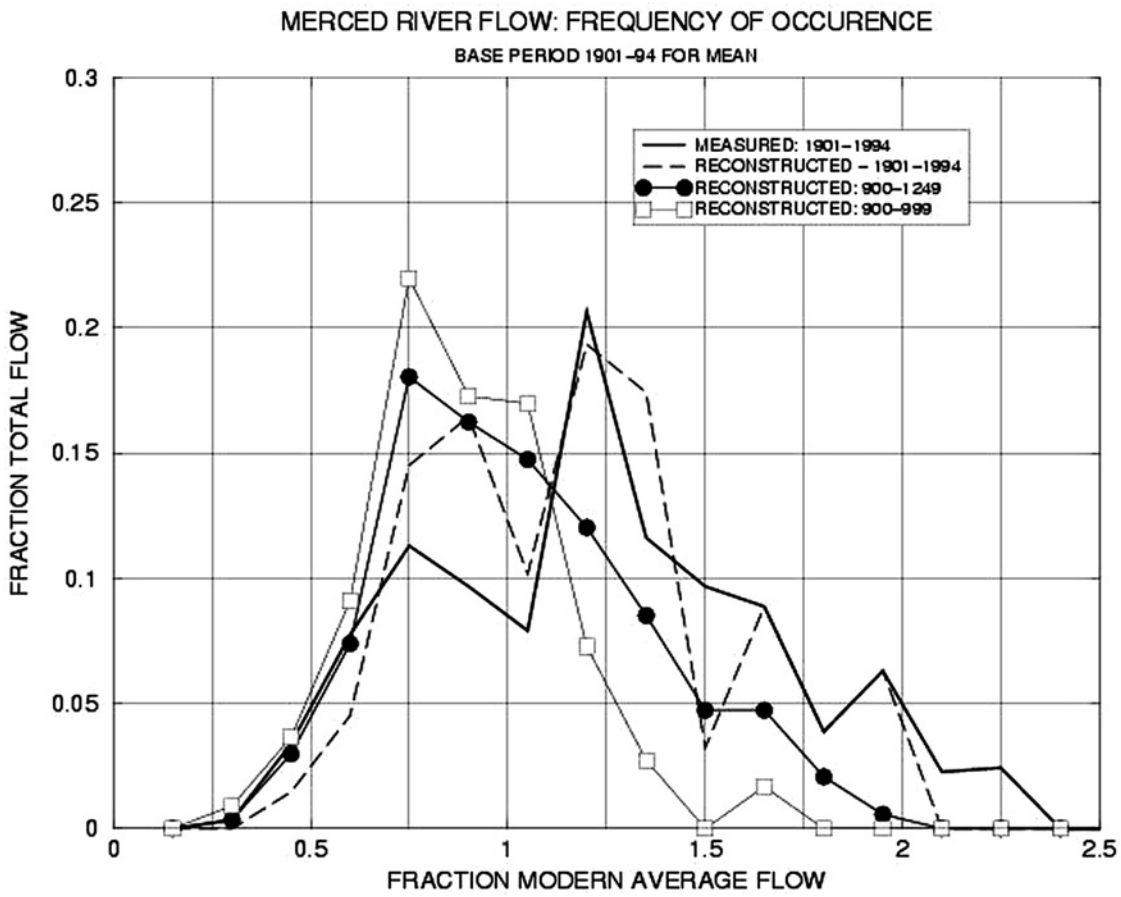

Figure 3 Frequency distributions of Merced River water-year flow (all as fractions of 1901–1994 mean, horizontal axis); measured flow for AD 1901–1994 (solid); reconstructed flow for 1901–1994 (dashed), reconstructed flow for AD 900–1249 (filled circles), and 900–999 (open squares)

decadal periods show conditions nearly as severe as during the first drought (reconstructed decadal means reaching 67% of the modern mean). Following the thirteenth-century flow minimum, the reconstructed record shows much less centennial variability than during earlier centuries and a steady increase (with the exception of a mild fifteenth-century decline) until early in the twentieth century.

The two periods of low flow during Mediaeval times are far more severe than any in the modern record (or in the complete reconstruction for that matter). For example, decadal-average Q_{MER} during the 1930s (the driest during historical times) reached just 71% of the observed long-term average (the reconstructed values reach 76% of that value), while the third most severe centennial average (during the fifteenth century) reached only as low as 90% of the modern average.

The differences between the modern and Mediaeval Merced River flow climatologies are made more apparent in the frequency distributions of measured and reconstructed flow in Figure 3. The contrast between the modern (AD 1901–1994) and MCA (AD 900–1249 and AD 900–999) distributions is stark, with the latter showing large reductions in the frequency of occurrence of years with flows above the modern average and large increases in the frequency of flows in the range 60–100% of that value. On a cumulative basis (not shown), reconstructed flows exceeding the modern observed flow median (95% of the mean) occur in only 15% the years during the tenth century and in just 32% of the years during the period AD 900–1249. The distributions in Figure 3 also emphasize that the MCA droughts were distinguished by the paucity of high flow years rather than the severity of individual very low-flow years. Over the AD 1900–1994 base period, the reconstruction underestimates the frequency of years with flows in the range from 50% to 70% of the modern average and overestimates those between 80% and 100% of the modern average. The distributions agree closely for higher flows, an important point for the Mono Lake simulations because high flow years account for most of the total flow volume (in the observed record, the upper 35% of annual flows accounts for half the total volume).

Comparisons with Mono Lake flow, precipitation, and evaporation data

To establish the soundness of using the Merced River data as a guide for Mono Lake inflow, Figure 4 shows a scatter plot of Q_{MER} versus the Mono Lake gauged Sierra Nevada runoff record (SNGR). Two features stand out in this comparison. First, there is a very close (R = 0.95) linear relationship between the two over the 47 years of overlap (1937–1983). The resulting relationship (given here in m^3), used later in the inflow reconstructions, is

$$SNGR' = 0.215\ Q_{MER} + 59.8 \times 10^6 \quad (2)$$

A second interesting feature in Figure 4 is that the relationship indicates a substantial 'base flow' component of SNGR amounting to 32% of its long-term mean value (59.8 million m^3/yr) if Merced River flow was reduced to zero.

The presence of this apparent 'base flow' in the SNGR record raises questions concerning how to reconstruct past Mono Lake inflow, so several other analyses were conducted to try to understand its character. One analysis examined the relationship between Mono Lake precipitation rate (MLPR) and SNGR. The

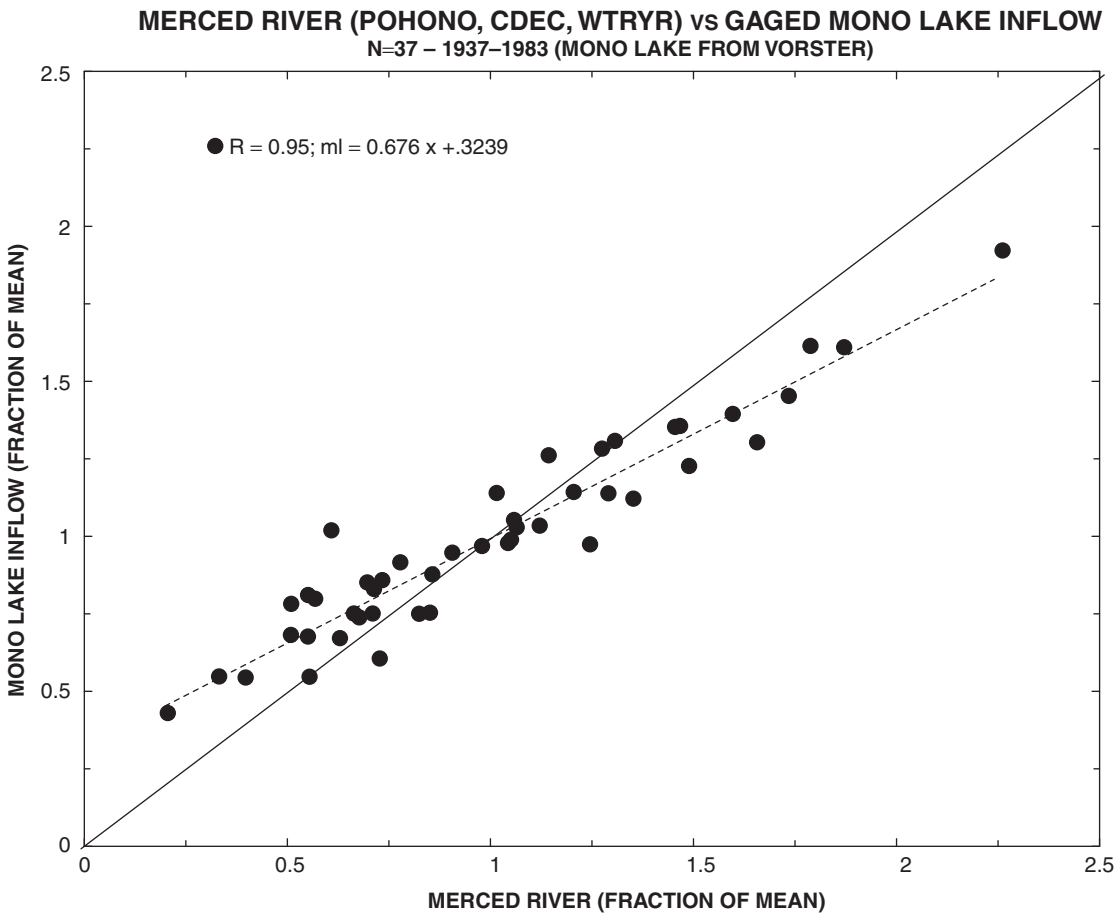

Figure 4 Mono Lake gauged Sierra Nevada runoff (SNGR; vertical axis) plotted as a function of Merced River Pohono Bridge discharge (Q_{MER}; horizontal axis). Data are for 1937–1983; both data sets are October–September water-year values plotted as fractions of respective means). Dashed line shows linear least-squares fit (R = 0.95); solid line shows one-to-one relation

relationship between these variables (not shown) gives a result similar to that in Figure 4, though with more scatter (R = 0.83), indicating the presence of a 'constant' base flow representing (about 30% of the mean).

In another analysis, the West Walker River (WWR) and SNGR records were compared. A scatter plot for these data (not shown) shows a strong linear relationship (R = 0.96; 1937–1983), and indicates a base flow (ie, for zero flow in the WWR) of 21% of mean SNGR. A comparison of the Q_{MER} and the WWR records gives a strong linear relationship (0.96; 1907–1994), indicating a WWR base flow 12% of average.

A final analysis concerning the SNGR base flow compares Yosemite Valley precipitation with Q_{MER}. This comparison (Figure 5) shows a very close linear relationship (R = 0.96) for the post-1920 period (data from earlier years suggest some spurious values), and indicates that Merced River flow annual flow would reach zero if precipitation was reduced to about 20 cm/yr (25% of the average). While this inference may not be correct, the pattern is in the opposite sense to that found at Mono Lake and argues against the presence of significant long-term base flow in the Merced River arising upstream of Yosemite Valley.

Together these analyses indicate that the SNGR record can be decomposed into one component that fluctuates in unison with Merced River flow and a second slowly varying (or constant) base flow component. The high correspondence between the fluctuating component and Merced River flow results from the fact that both derive from the runoff of annual precipitation at annual timescales. The second component, which apparently does not operate to an important degree in the Merced watershed, has timescales of variability of at least 50–100 years. This base flow apparently arises from percolation of snow melt and runoff through the fractured rock of the eastern slope of the Sierra Nevada (California Department of Water Resources, 1964), but the timescales on which it varies in response to changes in surface supply is not known.

The Mono Lake inflow reconstruction requires estimates of precipitation into the lake and onto surrounding land. Figure 6 shows a comparison between the SNDI record and the Mono Lake precipitation rate (MLPR) record. The relationship is a reasonably close non-linear relationship yielding the following quadratic regression equation (for units of m^3):

$$\text{MLPR'} = 0.0218\ \text{SNDI}^2 + 0.224\ \text{SNDI} + 1.848 \quad (3)$$

The correlation between the estimates from this regression and the actual MLPR record is 0.71 (1937–1983). This relationship is used to derive the precipitation component of Mono Lake inflow reconstructions used in the water balance model simulations described later.

It is worth considering whether changes in potential evaporation rate might have contributed significantly to the Mediaeval low stands. While no attempt to reconstruct potential evaporation has been undertaken here, some guidance concerning the relative magnitudes of their variability is available from the SNGR and MLPE records (Figure 7, both expressed as fractions of their 1937–1983 means). The most interesting result of this comparison is that the

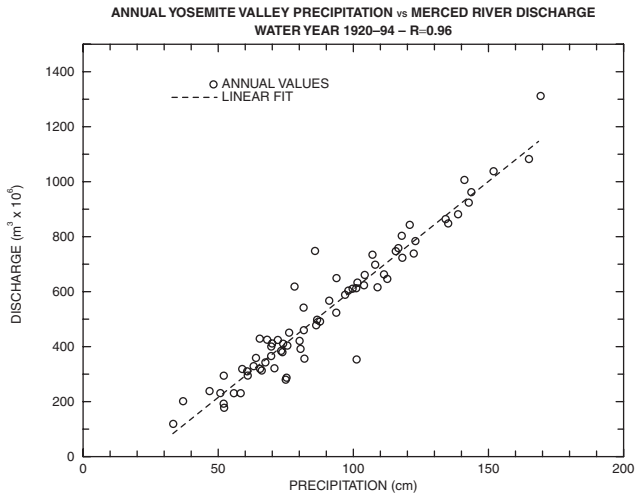

Figure 5 Water-year Merced River discharge plotted as a function of Yosemite Valley precipitation (circles); data for 1920–1994. Dashed line indicates linear regression fit ($R = 0.96$)

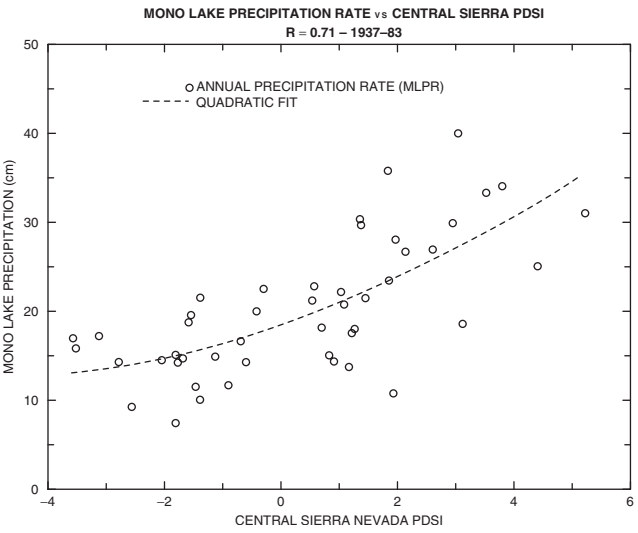

Figure 6 Mono Lake precipitation (vertical axis) plotted as a function of reconstructed PDSI Sierra Nevada Drought Index (horizontal axis) for 1937–1983; circles show annual values; dashed line shows quadratic fit

relative variability in MLPE ($\sigma = 0.07$) is less than that of SNGR ($\sigma = 0.31$) by a factor of four. A second feature of interest is that the association between the evaporation and runoff records is weak ($R = -0.38$) though significant at the 99% level. (The low lag-1 auto-correlations of 0.05 and 0.06 of the SNGR and MLPE records justify the use of a *t*-test with $n - 2$ (45) degrees of freedom for this significance test; the *a priori* assumption of a negative cross-correlation (based on earlier findings, see text below) justifies the use of a 1-tailed test (Sokal and Rohlf, 1973).)

Interestingly, the same correlation (–0.38) between precipitation and potential evaporation noted above is found in a data set constructed for California Climate Division 3 located on the east side of the northern Sierra Nevada in a setting similar to that of Mono Lake (Georgakakos and Smith, 2000). Further, a general tendency for a negative correlation between precipitation and pan evaporation has been documented both globally and in the US (Brutsaert and Parlange, 1998; Lawrimore and Peterson, 2000). While it is arguable whether these other findings are relevant to the relationship between Mono Lake SNGR and MLPE, the features in Figure 7 (if representative of those in past centuries) suggest that the Mediaeval Mono Lake low stands resulted primarily from changes in inflow (Sierra Nevada snowmelt and local precipitation), with variability in potential evaporation playing a secondary (and possibly constructive) role.

To further address the question of a possible role for evaporation rate changes in producing the Mono Lake low stands, experiments were conducted with the water balance model to investigate the relative sensitivity of simulated lake level to incremental changes in evaporation rate and precipitation. In one set of experiments, evaporation rate was held fixed (at the Vorster, 1985, MLPE value of 114.3 cm/yr) while total runoff (SNGR + USR + NSR) and lake precipitation (MLPR) were varied from 100% to 50% of the averages of the reconstructed values for 1900–1997 (see the section 'Mono Lake simulations', Method 1). In the other experiments, runoff and precipitation were held fixed at the 1900–1997 averages described above, while evaporation rate was varied from 100% to 160% of the Vorster (1985) MLPE value of 114.3 cm/yr (for comparison, note that the largest increase in estimated actual evaporation is only 10–15% (Figure 7)). For a given value of inflow (runoff and precipitation rate) and evaporation rate, the water balance model was run to equilibrium. The results of these sensitivity simulations (Figure 8) show that a reduction in inflow of 30% is required to reduce lake level by 16 m (to 1941 m, MSL). In contrast, evaporation rate must be increased by more than 50% to achieve the same reduction in lake level. This relative insensitivity of lake level to evaporation rate reflects the fact that total evaporation (volume) is a function of both evaporation rate and lake area, which decreases as lake volume decreases.

While the results discussed above (Figures 7 and 8) argue against a dominant role for changes in evaporation rate as a dominant factor in producing the Mediaeval low stands, we note that there is some evidence suggesting higher regional warm season temperatures during Mediaeval times (eg, Graumlich, 1993 and Lloyd and Graumlich, 1997 both from the Sierra Nevada, and Millar *et al.*, 2006 from the White Mountains, about 100 km southeast of Mono Lake), and this is consistent with the idea of increased potential evaporation rates.

Mono Lake simulations

Palaeosimulations of Mono Lake were conducted using two different inflow scenarios that attempt to cover much of the range of uncertainty in runoff discussed earlier. These inflow reconstructions differ in how the three runoff terms (SNGR, USR, NSR) are treated. In both inflow reconstructions, lake precipitation rate (MLPR) is modelled using the PDSI-based regression (Equation (3); Figure 6), and net land precipitation (NLSP) is assumed to fluctuate proportionally with MLPR, ie,

$$\mathrm{NLSP} = (\mathrm{MLPR} / \mathrm{MLPR_A}) * \mathrm{NLSP_A} \quad (4)$$

Where $\mathrm{MLPR_A}$ is the average for MLPR over the 1937–1983 period (20.32 cm/yr) and $\mathrm{NLSP_A}$ is the constant value used in Vorster (1985) for that same period (11.1×10^6 m^3/yr). MLPE (lake evaporation rate), BGE (bare ground evaporation) and other net losses are treated as described in the section 'Water budget and water balance model'.

For the first simulation (Method 1), total Mono Lake runoff (ie, from Sierran and non-Sierran sources, this is the sum of SNGR, USR and NSR) is reconstructed as directly proportional to fluctuations in reconstructed Merced River flow relative to the 1901–1994 measured mean,

$$\mathrm{MLR'} = (Q'_{\mathrm{MER}} / Q_{\mathrm{MERA}}) * (\mathrm{MLR_A}) \quad (5)$$

where Q'_{MER} is the reconstructed Merced River discharge defined in Equation (1), Q_{MERA} is average measured water-year Merced River discharge for 1901–1994, $\mathrm{MLR_A}$ is the average total Mono

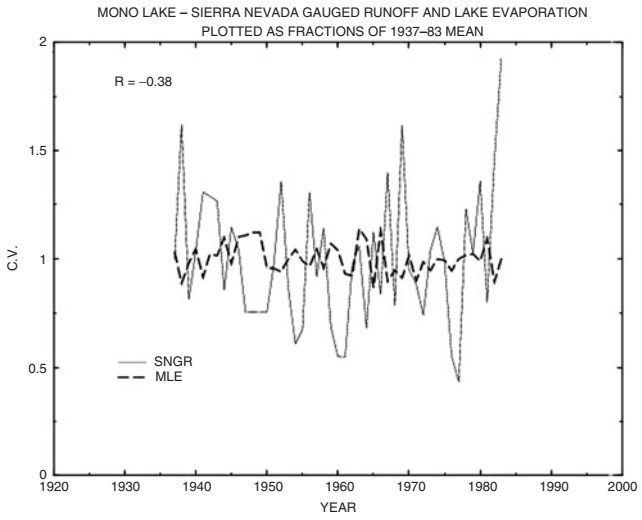

Figure 7 Coefficient of variability (value divided by 1937–1983 mean, C.V., vertical axis) for Mono Lake Sierra Nevada Gauged Runoff (SNGR; solid) and Mono Lake Evaporation (MLE; dashed)

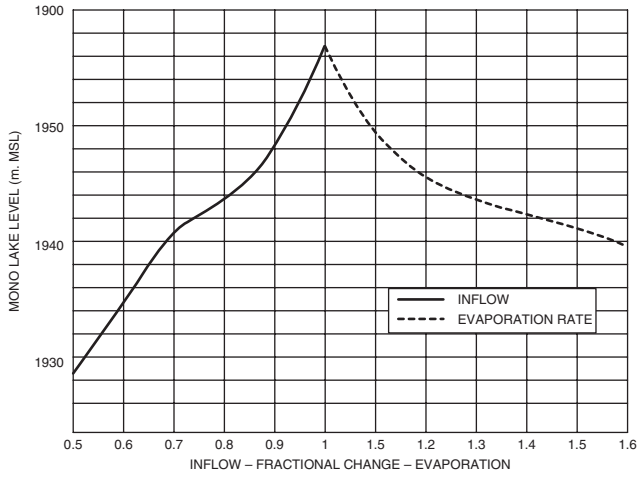

Figure 8 Sensitivity of simulated Mono Lake level (vertical axis) to fractional decreases in total inflow (values < = 1 on horizontal axis) and increases in evaporation rate (values > = 1 on the horizontal axis)

Lake runoff (SNGR+USR+NSR) for 1937–1983 and MLR' is the reconstructed total runoff.

The assumption behind the Method 1 approach is that essentially all components contributing to Mono Lake runoff, including the apparently 'constant' SNGR residual base flow and the percolation-driven NSR terms, are ultimately fed by precipitation associated with cool-season storms from the North Pacific. Following this assumption, over long (eg, multidecadal) timescales, total Mono Lake runoff would fluctuate in concert with runoff on the west side of the Sierra (Q_{MER}). Of course, even if these assumptions are correct, the approach does not include the impacts of delays and smoothing that would occur in the groundwater fractions of the runoff. Nevertheless, noting that the Mono Lake low stands had centennial timescales, and lacking information regarding the response of residual SNGR and NSR to surface runoff and precipitation variability (and assuming this is their source), the approach does not seem unreasonable.

The results of the Method 1 simulation (Figure 9) show an average twentieth-century level of 1957 m m.s.l., consistent with the 1958 m estimate for the modern 'natural level' given by Stine (1996; who references personal communication with P. Vorster). Most apparent in the simulation results are the two deep low stands during the tenth and thirteenth centuries, during which simulated lake levels dropped to approximately to 1943 and 1944 m m.s.l., respectively. These levels compare well with the 'no higher than' values of 1941 m m.s.l. for the two low stands given by Stine (1994). (Note: Stine (1994) gives 'no higher than' levels of 1941.5 and 1946 m m.s.l. for the two low stands, but recent evidence indicates that minimum lake level during the second low stand was lower than previously reported and very close to that of the first (Stine, personal communication, 2006).) The simulation results are in also in clear agreement with Stine's 'two low stand' scenario, and the timing (onset, termination, duration) agrees qualitatively with that given by Stine (1987, 1990, 1994). The magnitude of the lake level reductions are also consistent with Vorster (1985)-model-based calculations by Stine (1987, 1990) showing that steady-state total inflow values of 68% and 72% of modern values are required to bring simulated Mono Lake levels to equilibrium at 1941.5 and 1946 m m.s.l. levels. These values are consistent with the minimum decadal and centennial average reconstructed Merced River flows for the two drought periods reported in the section 'Merced River flow reconstruction' (60% and 75%, and 81% and 67%, respectively), and the delta-function inflow change response time of simulated lake level about 50 years.

A systematic inconsistency between the simulation results and the Stine (1994) scenario is that the simulated low stand terminations occur 75–100 years prior to the dates inferred from ^{14}C-derived 'death dates'. This discrepancy may arise in part from problems with the model forcing (eg, possible lags in the response of residual Sierra Nevada runoff (SNGR + USR) and NSR to precipitation variability; non-simulated potential evaporation variability), but the major contributing factor is thought to be bias in the ^{14}C age calibration.

For the second simulation (Method 2), only the SNGR fraction of the Mono Lake runoff terms was assumed to vary and was modelled using the regression equation given earlier (Equation (2); also see Figure 4). Thus, for this simulation, both the apparently near-constant fraction of total Sierra Nevada runoff (ie, 32% of SGNR+USR) and NSR were held constant. Precipitation was handled as in Method 1. As would be expected (because the variability time-dependent fraction of the inflow is smaller), the results (Figure 9) are (essentially) identical to those for Method 1 in terms of timing and show slightly higher (by 2–2.5 m) levels for the Mediaeval low stands.

Spatial extent of the Mediaeval Central Sierra Nevada droughts

The results presented to this point confirm Stine's (1987, 1991, 1994) scenario of two distinct Mediaeval Sierra Nevada droughts. We next consider these two droughts from a spatial perspective, addressing three questions. First, what was the spatial signature of these droughts? Were they local, regional, or did they cover the entire western USA? Were their spatial patterns similar? Second, were the spatial relationships associated with the Mediaeval Sierra Nevada droughts unusual, or do they recur after post-Mediaeval times? Third, are Mediaeval Sierra Nevada droughts typical of the general pattern of Mediaeval aridity in the western USA?

Reconstructed PDSI anomalies for AD 900–1009 and AD 1176–1274 (the droughts that produced the Mono Lake low stands, see Figure 2), are shown in Figure 10(A) and (B), respectively. The first drought extended from a core region in central and southern California into Arizona and northeast through the Great Basin and into Wyoming and Montana. For this drought, PDSI averages were near their long-term mean in Oregon and Washington, and show relatively moist conditions in British Columbia. This north–south dipole pattern in the far West is somewhat similar to that seen in analyses of precipitation changes associated with interannual and decadal shifts in North Pacific winter circulation (eg, those associated with El Niño activity and Pacific decadal variability; Mantua *et al*., 1997; Rajagopalan *et al*., 2000), although the northward extension through the Great Basin is not typical of patterns from the instrumental record

(see Graham *et al*., 2006). The second drought (Figure 10(B)) was less severe than the first, was again focused most extensively in central and southern California and in this instance extended northward through western Nevada and into Idaho. This second drought was thus confined more to the far western USA than the first. As in the first drought, conditions in the Pacific Northwest were near normal. In contrast to the first drought, reconstructed PDSI conditions in British Columbia were near normal.

To get an idea of which areas shared the particular two drought sequence associated with the Mono Lake low stands, a binary time series was created to represent the droughts with '1' for AD 900–1009 and for AD 1185–1274 and '0' for all other years (the time series covers AD 800–1990). Figure 10(C) shows the correlations between this binary record and 51-yr running mean gridded PDSI for AD 800–1990. The highest correlations (above 0.8) are centred over central and southern California, with values above 0.6 extending into Nevada and Arizona. As expected from Figure 10(A) and (B), there is some expression of a north–south dipole pattern (correlations over British Columbia reach 0.4) and little association over most of the Pacific Northwest. This result indicates that the pattern of precipitation deficits that produced the distinctive Mono Lake Mono Lake 'two low stand' signal was largely confined to California and western Nevada. To address the question of whether the 'teleconnection' pattern in Figure 10(C) holds for the post-Mediaeval period, we calculated correlations between the PDSI series at 37N 120W (that used to create the Merced River streamflow and Mono Lake inflow series) and gridded values elsewhere (all data low-passed with a 51-yr running mean) for the post-MCA period 1300–1990. The resulting pattern (Figure 10(D)) bears strong similarity to that in Figure 10(C), indicating that though the Mediaeval Sierra Nevada droughts were quite unusual in terms of severity, the associated spatial relationships were similar to those found for post-Mediaeval time.

The final issue is whether the Mediaeval Sierran droughts were 'typical' of the general pattern of aridity in Mediaeval western North America. In some senses, this question is poorly posed – these Sierran droughts did occur during Mediaeval times and are thus part of the general structure of Mediaeval climate in the region. Nevertheless, the typical pattern of drought and coherent drought variability over the West in Mediaeval times is concentrated over the Great Basin and extending into the western Great Plains (eg, Herweijer *et al*., 2006: figures 2 and 6; Graham *et al*., 2006: figure 5). This distinction probably relates most importantly to the annual cycle of precipitation that swings from being focused almost entirely from boreal winter half-year accumulations over the far west to a maximum in late spring and early winter over the western Plains (eg, Horn and Bryson, 1960; Hsu and Wallace, 1976). From this perspective, the Mediaeval Sierran droughts were distinct in that they reflect deficits in boreal winter half-year precipitation rather than the more prevalent pattern spring and early summer deficits that more generally characterize Mediaeval western USA drought.

Summary and conclusions

A water balance model driven with proxy-derived inflow estimates has been used to perform palaeosimulations of Mono Lake covering the past 2 kyr. The particular focus of the work is to attempt reconstruction of the Mediaeval low stands documented by Stine (1987, 1990, 1994, personal communication, 2006). The modelling methodology and many other aspects of the simulations follow the approach, considerations and data provided in Vorster (1985).

The lake modelling work was facilitated considerably by four facts:

(1) Mono Lake is a terminal lake in which volume changes result only from fluctuations in inflow (runoff and precipitation) and evaporation.
(2) Mono Lake inflow principally from runoff from Sierra Nevada snowmelt, and the much (possibly all) of the remainder also derives from North Pacific cool season storms.
(3) The discharge record for the Merced River, which drains the watershed on the west slopes of the Sierra opposite Mono Lake, fluctuates closely with Mono Lake Sierra Nevada runoff.
(4) Tree-ring data (from moisture-stressed trees on the west slopes of the Sierra Nevada) provide a relatively accurate reconstruction of cool-season precipitation and snowmelt driven streamflow.

Tree-ring data (from the gridded drought severity reconstruction of Cook *et al*., 2004) were used to reconstruct snowmelt-fed streamflow on the western slope of the central Sierra Nevada and this record was converted to reconstructed Mono Lake runoff. The same tree-ring data were used to reconstruct precipitation for Mono Lake (a secondary, but important, term in lake water balance). The reconstructed runoff and precipitation were then used to drive an implementation of the Vorster (1985) Mono Lake water balance model. The results of the simulations were then compared with the findings of Stine (1994) with respect to severe Mediaeval droughts and the resultant Mono Lake low stands.

An important element of the study is a reconstruction of Merced River flow. This reconstruction shows two severe centennial-scale droughts during the MCA at approximately the same time as the Mono Lake low stands. The Merced River annual streamflow deficits during these Mediaeval droughts were far more severe than anything experienced during historic times, and have not been closely approached in the past 550 years, with (reconstructed) centennial average flow reaching 75% of modern annual averages and decadal averages reaching 60% of that value. In comparison, during the most severe drought in the observed record, decadal average discharge reached 75% of the 1901–1994 mean. It is also shown that the Mediaeval droughts (as they appear in the flow reconstruction) were marked more by the paucity of years with near-normal flow than by the magnitude of flow deficits in a relatively few dry years. This emphasizes the fact that centuries of Mediaeval drought were apparently characterized by a marked and persistent change (relative to today) in winter circulation patterns over the North Pacific and North America, as surmised by Stine (1994; c.f. Cobb *et al*., 2003; Herweijer *et al*., 2006; Graham *et al*., 2006).

Some secondary findings of interest that influenced the way simulations were conducted and interpreted include the following.

(A) The association between fluctuations in the relatively short (47-yr) record of measured Sierra Nevada runoff for Mono Lake (SNGR) and that of Merced River discharge is very close (correlation of 0.95).
(B) There is clear evidence that the SNGR record is made up of two components – one that fluctuates closely on interannual timescales with Merced River flow, and a second 'base flow' component that has much longer timescales of variability.
(C) Two lines of evidence suggest that the importance of changes in potential evaporation in contributing to the Mono Lake low stands was secondary. First, the variability in Mono Lake potential evaporation (as calculated for 1937–1983 in Vorster, 1985) is much lower in magnitude than the variability in Mono Lake inflow (Figure 7). Second, lake level is less sensitive to large changes in evaporation rate than to like-sized reductions in inflow (see Figure 8 and related discussion).

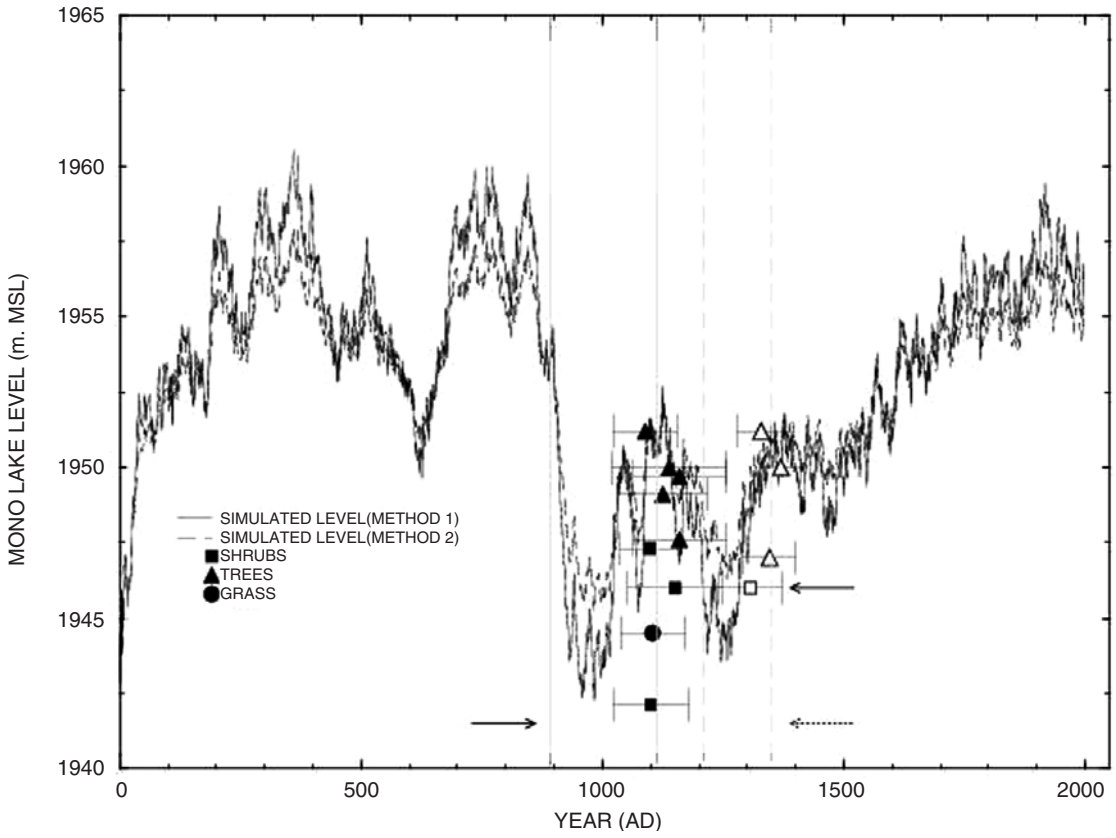

Figure 9 Simulated Mono Lake level using Method 1 (black line) and Method 2 (dashed line). Symbols show elevation and calibrated 14C 'death dates' (from Stine, 1994) for trees (triangles), shrubs (squares) and grass (circle) with 1 σ uncertainties (bars) for the Mono Lake low stands. Grey solid (dashed) lines mark the nominal low stand durations (from Stine,1994) and solid arrows mark the 'no higher than' low stand lake levels from Stine (1994); dashed arrow marks the estimated level of the second low stand from more recent work (S. Stine, personal communication, 2006)

The results of the Mono Lake palaeosimulations show two deep low stands that agree closely in magnitude and timing with those inferred from the relic vegetation by Stine (1994). The main systematic discrepancy is that the simulated low stands end 75–100 years prior to the calibrated ^{14}C death dates of the relic trees and shrubs. This discrepancy probably arises in part from problems with the modelling (eg, incorrect handling of base flow, lack of variability in potential evaporation, errors in the Merced River reconstruction), but is thought to be due primarily to bias in the calibration of the ^{14}C ages of the fossil vegetation.

The spatial distributions of the two Mediaeval Sierra Nevada droughts (as seen in the reconstructed PDSI data) show that both were focused over central and southern California. The first, and more severe, drought extended north and east across the Great Basin into the northern Rocky Mountains and had an opposing signal of moist conditions over British Columbia. In contrast, the second drought was less severe, confined to the far western USA and shows no signal over British Columbia. Neither drought shows much signal over the Pacific Northwest. Further analysis emphasizes that the distinctive 'two drought' Mono Lake low stand signal was confined largely to central and southern California and western Nevada. This pattern of teleconnection correlations is closely reproduced using post-1300 data only, showing that while the Mediaeval Sierran droughts were distinctive in their persistence and severity, the teleconnection pattern is typical of multidecadal variability during the past seven centuries. A final discussion points out that the 'Mono Lake droughts' were distinctive for their over-California focus and thus for major deficits in boreal winter precipitation. The more general pattern of coherent Mediaeval aridity in the western USA was focused over the Great Basin and western Plains and likely resulted largely from spring and early summer precipitation deficits. These results council caution in necessarily drawing close comparison between the specific timing of the Mono Lake low stands with patterns of Mediaeval climate change elsewhere.

Overall, the results represent a useful step forward in that they provide strong independent corroborative evidence for the occurrence and magnitude of the Mono Lake low stands, and place some quantitative bounds on the severity and duration of central Sierra Nevada streamflow reductions during Mediaeval times. At the same time, the reconstructed streamflow results do not directly account for the presence of relict stumps near the bottom of the valley of the West Walker River (60 km north of Mono Lake) or those rooted approximately 21 m below the present surface of Tenaya Lake in the Sierra Nevada about 35 km west of Mono Lake. As described by Stine (1987, 1990, 1994), ^{14}C ages of the relict trees from both these sites fall into two groups consistent with those from Mono Lake, with the Tenaya Lake tree-ring ages suggesting low stand durations of at least 140 and 100 years, respectively. As pointed out by Stine (1987, 1990, 1994), the presence of long-lived relict stumps of inundation-intolerant trees at these sites (each of which is much more sensitive to annual runoff fluctuations than is Mono Lake) argues that severe drought conditions persisted for many decades without break during the MCA. This apparently clear evidence is at odds with the central Sierra tree-ring PDSI record used in this study, which indicates that some experienced above modern-average precipitation during both periods of centennial aridity. Reconciling this inconsistency presents an important challenge for the description of the range of late-Holocene climate variability in the central Sierra Nevada.

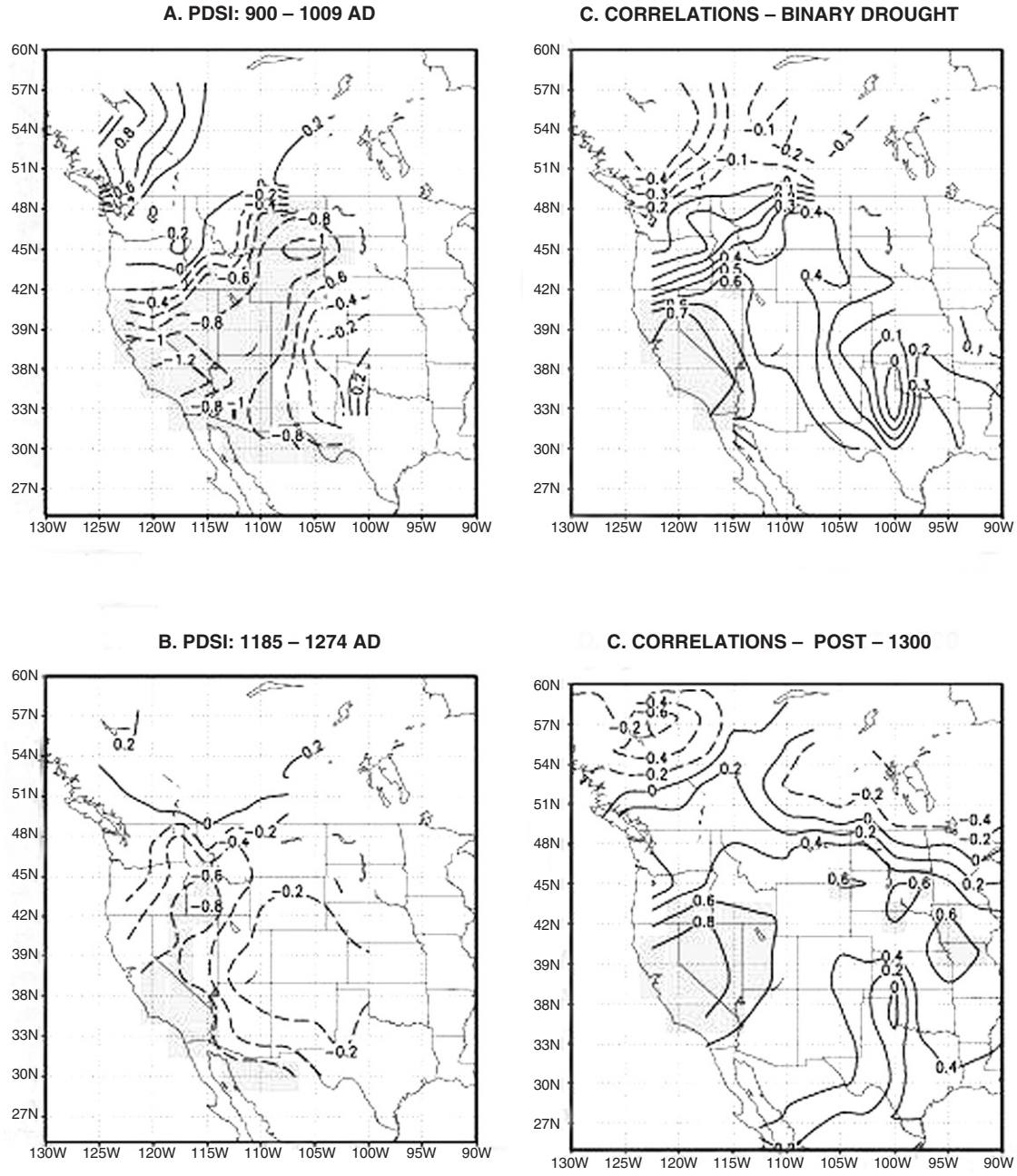

Figure 10 (A) and (B) Reconstructed PDSI anomalies for AD 900–1009 and AD 1185–1274 (with respect to 800–1990 averages); contour interval is 0.2, values less than –0.6 are shaded. (C) Correlations with binary 'drought–no drought' record and 51-yr running average gridded PDSI for AD 800–1990 (see text); contour interval is 0.1; values greater than 0.6 are shaded. (D) Correlations between gridded PDS series at 37N 120W and all other grid points for 51-yr running average data from AD 1300 to 1990. Contour interval is 0.2; values greater than 0.6 are shaded. Reconstructed PDSI data are from Cook *et al*. (2004)

Acknowledgements

This work was supported by the NSF Earth System History program under NSF Grant ATM0213962 to MKH, NOAA Grant (NA06OAR4310120) to NEG, by the California Energy Commission PIER Program through the California Climate Change Center at Scripps Institution of Oceanography. The authors are grateful for helpful comments from L. Benson and for many useful suggestions and careful reviews from S. Stine and P. Vorster.

Appendix A

Natural configuration of Mono Lake water balance model

The following changes in the terms above were made to configure the Vorster (1985) model for a setting prior to major human impacts.

(A) Bare ground evaporation is set to 16.4×10^6 m^3 (13.3×10^3 acre-feet), a value appropriate for relatively low lake levels.

(B) Evaporation from Grant Lake Reservoir is reduced to 36% of the nominal modern value in accordance with ratio of the areas of the modern lake (1100 acres) to the historically recorded area of the lake and wetland before construction of Grant Lake (400 acres). The 'natural' value is set at 0.64×10^6 m^3 (0.52×10^3 acre-feet).

(C) Historical data suggest that riparian vegetation was more extensive before diversion of the creeks flowing into Mono Lake. Guided by information in Vorster (1985), riparian evapotranspiration is increased to 2.71×10^6 m^3 annually (2.20×10^3 acre-feet).

(D) Losses to pasture irrigation and Mono Crater Tunnel are eliminated.

(E) Annual losses to phreatophyte evapotranspiration were reduced by 33% to account for a reduction in growth around irrigation channels; the new values are 2.64×10^6 m^3 annually (2.14×10^3 acre-feet).

(F) Contributions from municipal water and the Virginia Creek diversions are eliminated.

References

Anderson, R.S. and **Smith, S.J.** 1997: The sedimentary record of fire in Montane Meadows, Sierra Nevada, California, USA. In Clarke, J., Cachier, H., Goldammer, J.G. and Stocks, B., editors, *Sediment records of biomass burning and global change*. NATO ASI Series, Springer, 313–28.

Arbogast, A.F. 1996: Stratigraphic evidence for late-Holocene aeolian sand mobilization and soil formation in south-central Kansas, USA. *Journal of Arid Environments* 34, 403–14.

Benson, L., Kashgarian, M., Dye, R., Lund, S., Paillet, F., Smooth, J., Kester, C., Mensing, S., Meko, D. and **Lindström, S.** 2002: Holocene multidecadal and multicentennial droughts affecting Northern California and Nevada, *Quaternary Science Reviews* 21, 659–82.

Brutsaert, W. and **Parlange, M.B.** 1998: Hydrologic cycle explains the evaporation paradox. *Nature* 396, 30.

Byrne, R., Ingram, B.L., Starratt, S., Malamud-Roam, F., Collins, J.N. and **Conrad**, **M.E.** 2001: Carbon isotope, diatom, and pollen evidence for late Holocene salinity change in a brackish marsh in the San Francisco estuary. *Quaternary Research* 55, 66–76.

California Department of Water Resources 1964: *Groundwater occurrence and quality in the Lahontan Region*. California Department of Water Resources, 345–56.

Cobb, K.M., Charles, C.D., Cheng, H. and **Edwards**, **R.L.** 2003: El Niño/Southern Oscillation and tropical Pacific climate during the last millennium. *Nature* 424, 271–76.

Cook, E.R., Meko, D.M., Stahle, D.W. and **Cleaveland, M.K.** 1996: Tree-ring reconstructions of past drought across the coterminous United States: tests of a regression method and calibration/verification results. In Dean, J.S., Meko, D.M. and Swetnam, T.W., editors, *Tree rings, environment, and humanity, 17–21, May 1994, Tucson, Arizona*. Radiocarbon, 155–69.

—— 1999: Drought reconstructions for the continental United States. *Journal of Climate* 12, 1145–62.

Cook, E.R., Woodhouse, C., Eakin, C.M., Meko, D.M. and **Stahle, D.W.** 2004: Long-term aridity changes in the western United States. *Science* 306, 1015–18.

Georgakakos, K.P. and **Smith, D.E.** 2001: 'Soil moisture tendencies into the next century for the conterminous United States. *Journal of Geophysical Research – Atmospheres* 106, 27 367–82.

Graham, N.E., Hughes, M.K., Ammann, C.M., Cobb, K.M., Hoerling, M.P., Kennett, D.J., Kennett, J.P. Rein, B., Stott, L., Wigand, **P.E.** and **Xu, T.** 2006: Tropical Pacific–mid-latitude teleconnections in Medieval times. *Climatic Change* 83, 241–85.

Graumlich, L.J. 1993: A 1000-year record of temperature and precipitation in the Sierra Nevada. *Quaternary Research* 39, 249–55.

Harding, S.T. 1965: *Recent variations in the water supply of the Great Basin*. Archives Research Series Report 16, University of California, Berkeley.

Herweijer, C., Seager, R. and **Cook, E.R.** 2006: North American droughts of the mid-to-late nineteenth century: a history, simulation and implication for Medieval drought. *The Holocene* 16, 159–71.

Herweijer, C., Seager, R., Cook, E.R. and **Emile-Geay, J.** 2006: North American droughts of the mid to late nineteenth century: a history, simulation and implication for Mediaeval drought. *The Holocene* 16, 159–71.

Horn, L.H. and **Bryson, R.A.** 1960: Harmonic analysis of the annual march of precipitation over the United States. *Annals of the Association of American Geographers* 50, 157–71.

Hsu, C.-P. and **Wallace, J.M.** 1976: The global distribution of the annual and semiannual cycles in precipitation. *Monthly Weather Review* 104, 1093–101

Hughes, M.K. and **Funkhouser, G.** 1998: Extremes of moisture availability reconstructed from tree-rings from recent millennia in the Great Basin of Western North America. In Beniston, M. and Innes, J.L., editors, *Impacts of climate variability on forests*. Berlin, 99–107.

Hughes, M.K. and **Graumlich, L.J.** 1996: *Climatic variations and forcing mechanisms of the last 2000 years*. NATO ASI Series, Vol. 141, Multi-millennial dendro-climatic studies from the western United States, 109–24.

LaMarche, V.C. 1974: Paleoclimatic inferences from long tree-ring records. *Science* 183, 1043–88.

Lawrence, D.B. and **Lawrence, E.G.** 1961: Response of enclosed lakes to current glaciopluvial climatic conditions in middle latitudes Western North America. *Annals of the New York Academy of Science* 95, 341.

Lawrimore, J.H. and **Peterson, T.C.** 2000: Pan evaporation trends in the dry and humid regions of the United States. *Journal of Hydrometeorology* 1, 543–46.

Lloyd, A.H. and **Graumlich, L.J.** 1997: Holocene dynamics of treeline forests in the Sierra Nevada. *Ecology* 78, 1199–210.

Mantua, J.N., Hare, S.R., Zhang, Y., Wallace, J.M. and **Francis, R.C.** 1997: A Pacific interdecadal oscillation with impacts on salmon production. *Bulletin of the American Meteorological Society* 78, 1069–80.

Mehringer, P.J. and **Wigand, P.E.** 1990: Comparison of Late Holocene environments from woodrat middens and pollen: Diamond Craters, Oregon. In Betancourt, J.L., Van Devender, T.R. and Martin, P.S., editors, *Fossil packrat middens: the last 40,000 years of biotic changes*. University of Arizona Press, 294–325.

Meko, D.M., Cook, E.R., Stahle, D.W., Stockton, C.W. and **Hughes, M.K.** 1993: Spatial patterns of tree-growth anomalies in the United States and southeastern Canada. *Journal of Climate* 6, 1773–86.

Meko, D.M., Therrell, M.D., Baisan, C.H. and **Hughes, M.K.** 2001: Sacramento river flow reconstructed to A.D. 869 from tree rings. *Journal of the American Water Resource Association* 37, 1029–39.

Millar, C.I., King, J.C., Westfall, R.D., Alden, H.A. and **Delany, D.L.** 2006: Late Holocene forest dynamics, volcanism and climate change at Whitewing Mountain and San Joaquin Ridge, Mono County, Sierra Nevada, CA, USA. *Quaternary Research* 66, 273–87.

Mohr J.A., Whitlock, C. and **Skinner, C.N.** 2000: Postglacial vegetation and fire history, eastern Klamath Mountains, California, USA. *The Holocene* 10, 587–601.

Rajagopalan, B., Cook, E., Lall, U. and **Rey, B.K.** 2000: Spatiotemporal variability of ENSO and SST teleconnections to summer drought over the United States during the 20th century. *Journal of Climatology* 13, 4244–55.

Sokal, R.R. and **Rohlf, F.J.** 1973: *Introduction to biostatistics*. W.H. Freeman and Company.

Stine, S. 1987: Mono Lake: the past 4,000 years. Ph.D. dissertation, University of California, Berkeley, 615 pp.

—— 1990: Late Holocene fluctuations of Mono Lake, eastern California. *Palaeogeography, Palaeoclimatology, Palaeoecology* 78, 333–81.

—— 1994: Extreme and persistent drought in California and Patagonia during Mediaeval time. *Nature* 369, 546–49.
—— 1996: Climate of the Sierra Nevada, 1650–1850. In *Sierra Nevada Ecosystem Project, final report to Congress, v. 2: assessments and scientific basis for management options*. Regents of the University of California, 25–30. Accessed 20 September 2007 from http://ceres.ca.gov/snep/pubs/web/PDF/VII_C02.PDF
—— 1998: A Medieval climatic anomaly in the Americas. In Issar, A. and Brown, N., editors, *Water, environment and society in times of climatic change*. Kluwer Academic Publishers, 43–67.
Stockton, C.W. and **Meko, D.M.** 1975: A long-term history of drought occurrence in western United States as inferred from tree-rings. *Weatherwise* 28, 244–49.
Swetnam, T.W. 1993: Fire history and climate change in Giant Sequoia Groves. *Science* 262, 885–89.
Vorster, P. 1985: *A water balance forecast model for Mono Lake, California*. United States Department of Agriculture, Forest Service Region 5, Earth Resource Monograph 10, 350 pp. Available from United States Forest Service, Southwest Region, 1323 Club Drive, Vallejo, CA 94592, USA (retrieved 20 September 2007 from http://www.monobasinresearch.org/onlinereports/deirap.htm).
Yuan, F., Linsley, B.K., Lund, S.P. and **McGeehin, J.P.** 2004: A 1200 year record of hydrologic variability in the Sierra Nevada from sediments in Walker Lake, Nevada. *Geochemistry, Geophysics and Geosystems* 5, 2004 doi:10.1029/2003GC000652.